Thermal radiation in quasiperiodic photonic crystals with negative refractive index

2007 J. Phys.: Condens. Matter 19 496212

(http://iopscience.iop.org/0953-8984/19/49/496212)

IOP PUBLISHING JOURNAL OF PHYSICS: CONDENSED MATTER

J. Phys.: Condens. Matter **19** (2007) 496212 (13pp) doi:10.1088/0953-8984/19/49/496212

Thermal radiation in quasiperiodic photonic crystals with negative refractive index

F F de Medeiros[1], E L Albuquerque[1], M S Vasconcelos[2] and P W Mauriz[2]

[1] Departamento de Física, Universidade Federal do Rio Grande do Norte, 59072-970 Natal-RN, Brazil
[2] Departamento de Ciências Exatas, Centro Federal de Educação Tecnológica do Maranhão, 65025-001 São Luís-MA, Brazil

Received 4 September 2007, in final form 16 October 2007
Published 15 November 2007
Online at stacks.iop.org/JPhysCM/19/496212

Abstract

In this work we investigated the thermal power spectrum of the electromagnetic radiation through one-dimensional stacks of alternating negative and positive refractive index layers, arranged as truncated quasiperiodic photonic structures obeying the Fibonacci (FB), Thue–Morse (TM), and double-period (DP) sequences. The thermal radiation power spectra are determined by means of a theoretical model based on a transfer matrix formalism for both normal and oblique incidence geometries, together with Kirchoff's second law. We studied the radiation spectra by considering the case where both refractive indices of layers A and B are assumed to be a constant, as well as a more realistic case which takes into account the frequency-dependent electric permittivity ϵ and magnetic permeability μ to characterize the negative refractive index n in layer B.

1. Introduction

Materials with simultaneously negative permittivity ϵ and negative permeability μ, yielding a negative refractive index n (i.e. the negative square root $n = \sqrt{\epsilon\mu}$ had to be chosen), the so-called negative index materials (NIMs) or metamaterials, have recently been extensively studied in several distinct artificial physical settings, inspired by Veselago's work [1] many years ago. However, Veselago's work was mainly an academic curiosity for a long time, as real materials with negative ϵ and μ were not available. This situation changed when theoretical proposals demonstrated that it is possible to obtain both negative ϵ and μ, within a certain frequency domain, if metallic periodically structured photonic media (microwave materials) are used [2], bringing Veselago's result into the limelight. Further, the striking demonstration by Pendry [3] that NIM can be used to make perfect lenses with resolution capabilities not limited by the conventional diffraction limit, has given an enormous boost to the interest in these materials. Experimentally, they were achieved for structures fabricated by interspersing effective media ϵ (thin metal wires or electric resonators) with effective media

μ (magnetic resonators such as split rings or high dielectric fibers) [4, 5]. Besides, negative refraction phenomena can also occur in other situations, such as in materials with strong dispersion and losses [6, 7].

Several schemes for their fabrication have been proposed or realized so far, in which they exhibit both electric and magnetic resonances that can be separately tuned to occur from megahertz to terahertz frequency bands, and hopefully to the visible region of the electromagnetic spectrum (for a review see [8] and references cited therein). Furthermore, a number of applications making use of metamaterials have been proposed. For instance, Tassin and collaborators introduced ideas for 1D cavity resonators utilizing the concept of lossless metamaterials in which both the permittivity ϵ and the permeability μ possess negative real values at given frequencies, opening up the possibility of having subwavelength thin compact cavity resonators [9]. Such subwavelength cavity resonators can lead to very interesting designs for various compact subwavelength devices and components. Flat lenses with arbitrary index of refraction and arbitrary characteristic impedance were also proposed, retaining some useful properties such as three-dimensional imaging, lack of spherical aberrations, easy manufacturing, and invariance of the optical axis [10].

Negative refraction occurs at interfaces as a natural consequence of the negative group velocity of waves in one of the interfacing media. The origin of this understanding has been discussed by Agranovich and Gartstein [11] by using a framework where the generalized dielectric tensor $\epsilon_{ij}(\omega, k)$ represents the electromagnetic response of the metamaterial medium to perturbations of frequency ω and wavevector k, with a sufficiently strong spatial dispersion. However, the dependence of the electric (magnetic) permittivity (permeability) on the wavevector (spatial dispersion) is not an intrinsic property of metamaterials, since it may appear also in semiconductors in the exciton–polariton regime. They are mixing modes formed by the interaction between the exciton (the electron–hole pair) and the photon in the band-gap frequency region between the valence and the conduction band, where the k-dependence of the dielectric function gives rise to a rich phenomenology when compared to the corresponding phonon–polaritons. One of the main consequences of the spatial dispersion is the existence of two transversal and one longitudinal mode for the bulk exciton–polariton dispersion relation, give rising to a 'bottle neck' like profile when k goes to zero [12]. We believe that a similar effect could occur when we consider the spatial dispersion in metamaterials.

One of the main consequences of NIMs is that the electric field $\vec{E}$, the magnetic field $\vec{H}$, and the wavevector $\vec{k}$ form a left-handed triplet. Due to that, NIMs are sometimes referred to as left-handed materials (LHM), which is adopted here from now on, because they support 'backward waves', i.e. waves with the phase velocity opposite to the direction of the energy flow. Assuming the direction of the energy flux as positive, they also present a negative phase velocity [13]. Moreover, their phase and group velocities are antiparallel, since usually the group velocity has the same direction as the Poynting vector.

The great success of LHM is justified by their technological use with novel properties, such as magnetic resonance imaging (MRI) using radio frequency magnetic field to excite the nuclear spins in a patient's body [14], and in the development of new types of radio-antennas [15], to cite just a few. One of the most studied group of LHM are the so-called metamaterials, based on current-conducting elements made up of wires and loops that have inductive and capacitive characteristics (for a recent review see [16]). While the wires assume an effective negative electrical permittivity, the various loops provide a negative magnetic permeability in the same frequency band [17]. On the other hand, photonic crystals represent also an alternative way to attaining negative refraction, whose optical band structure is analogous to the electronic band structure in a solid [18]. Moreover, they have less loss to optical frequencies than the metamaterials based on conducting elements [19].

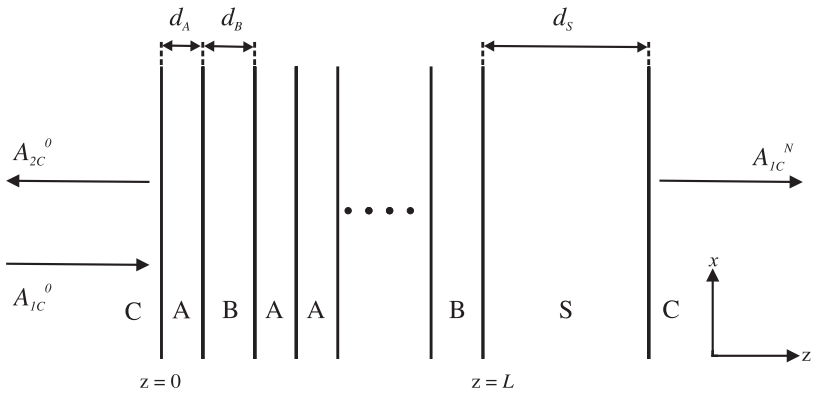

Figure 1. The geometrical schematic representation of the multilayered photonic band-gap structure considered in this work. The layers A and B have thicknesses d_A and d_B, respectively, while L is the size of the whole quasiperiodic structure grown on an absorbing substrate of thickness d_S. We choose the medium C as a vacuum, in which the total structure is embedded.

Until recently, no comprehensive analysis of the influence of the LHM to the thermal radiation distribution appeared in the literature. There are few papers dealing with the quantum field description of LHM related phenomena, such as the modification of spontaneous emission and the super-radiance effect [20]. Recently, Maksimović *et al* [21] analyzed the modification of thermal radiation when it passed over a periodic and quasiperiodic (Cantor) multilayer structure incorporating both LHM and conventional materials for both s- and p-polarizations. They showed that thermal radiation spectra are strongly influenced by structures containing LHM in comparison to all-positive refractive index multilayered structures.

It is the aim of this work to investigate the behavior of a light beam normally and obliquely incident on a one-dimensional multilayer photonic structure, composed of SiO_2/LHM layers arranged in a quasiperiodical fashion, which follows the Fibonacci (FB), Thue–Morse (TM), and double-period (DP) substitutional sequences (for an up to date review of these quasiperiodic structures see [22]). The main reason for studying these structures is that they are realizable experimentally, so they are not mere academic examples of a quasicrystal. These quasiperiodic structures can be generated by their inflation rules, as follows: $A \to AB$, $B \to A$ (FB); $A \to AB$, $B \to BA$ (TM); $A \to AB$, $B \to AA$ (DP). Here, A (thickness d_A) and B (thickness d_B) are the building blocks modeling the SiO_2 and LHM layers, respectively. We use a theoretical model based on Kirchoff's second law to calculate the emission spectra of the thermal radiation in these multilayered structures, together with a transfer matrix formalism, which simplifies enormously the algebra involved in the calculation.

The outline of this paper is as follows. In section 2 we present the theoretical calculation based on the transfer matrix method together with the thermal radiation spectra in multilayered photonic structures. The numerical results are discussed in section 3, while the conclusions are summarized in section 4.

2. General theory

Consider the quasiperiodic multilayer structure, as depicted in figure 1. Medium A, with thickness d_A, is fulfilled by SiO_2, and is characterized by a positive refractive index $n_A = \sqrt{\epsilon_A \mu_A}$ and an impedance $Z_A = \sqrt{\mu_A/\epsilon_A}$, both constants. Medium B is a metamaterial with thickness d_B, and is characterized by a negative refractive index $n_B = \sqrt{\epsilon_B \mu_B}$ and an

impedance $Z_B = \sqrt{\mu_B/\epsilon_B}$. The multilayer structure is grown on an absorbing substrate S, with a constant refractive index n_S. The entire structure is embedded in a transparent medium C (considered to be air or vacuum) with a constant refractive index n_C.

To calculate the spectral properties of the one-dimensional optical quasiperiodic structures, i.e. the Fibonacci, Thue–Morse and doubled-period sequences, we can use a transfer matrix method [23]. This method consists of relating amplitudes of the electromagnetic fields in a layer with those of the previous layer, and so on, by successive applications of Maxwell's electromagnetic boundary conditions at each interface along the multilayer system. Therefore, the transfer matrix relates the electromagnetic incident field amplitudes (A^0_{1C} and A^0_{2C}) of one side of the multilayer system (at $z < 0$), with the transmitted amplitude A^N_{1C} of the electromagnetic field in the other side, at $z > L$, L being the size of the multilayer system (see figure 1), by means of the product of the interface matrices $M_{\alpha\beta}$ (α, β being any A, B, S and C media) and the propagation matrices M_γ ($\gamma = A$, B and S), as follows [24]:

$$\begin{pmatrix} A^0_{1C} \\ A^0_{2C} \end{pmatrix} = M_{CA} M_A M_{AB} M_B \cdots M_{BS} M_S M_{SC} \begin{pmatrix} A^N_{1C} \\ 0 \end{pmatrix}, \tag{1}$$

where

$$M_{\alpha\beta} = \tfrac{1}{2} \begin{pmatrix} 1 + Z_\alpha/Z_\beta & 1 - Z_\alpha/Z_\beta \\ 1 - Z_\alpha/Z_\beta & 1 + Z_\alpha/Z_\beta \end{pmatrix}, \tag{2}$$

$$M_\gamma = \begin{pmatrix} \exp(-\mathrm{i}k_\gamma d_\gamma) & 0 \\ 0 & \exp(\mathrm{i}k_\gamma d_\gamma) \end{pmatrix}, \tag{3}$$

with $k_\gamma = n_\gamma \omega/c$.

The above matrices were obtained for the normal incidence case. For the oblique incidence case, we need to replace $Z_\alpha \to Z_\alpha/\cos\theta_\alpha$ for s-polarization or TE mode, and $Z_\alpha \to Z_\alpha \cos\theta_\alpha$ for p-polarization or TM mode in the interface matrices, as well as $n_\gamma \to n_\gamma \cos\theta_\gamma$ for both TE and TM polarizations in the propagation matrices.

The transmittance and the reflectance coefficients are simply given by

$$R(\omega) = \left| \frac{M_{21}}{M_{11}} \right|^2 \qquad \text{and} \qquad T(\omega) = \left| \frac{1}{M_{11}} \right|^2, \tag{4}$$

where $M_{i,j}$ ($i, j = 1, 2$) are the elements of the optical transfer matrix $M(\omega) = M_{CA} M_A M_{AB} M_B \cdots M_{BS} M_S M_{SC}$. If no absorbing material is introduced in the multilayer system, i.e. if the refractive indices are all real (lossless), then $R(\omega)+T(\omega) = 1$ by conservation of energy. When we introduce a material with complex refractive index, i.e. the absorption is present, $R(\omega)$ and $T(\omega)$ can be used to define a real absorptance by $A(\omega) = 1 - R(\omega) - T(\omega)$, which is again a statement of conservation of energy. However, from Kirchoff's second law, we know that the ratio of the thermal emittance $E(\omega)$ to the absorptance $A(\omega)$ is a constant, independent of the nature of the material, being unity when the source is a perfect blackbody [25, 26]. Hence, $E(\omega) = A(\omega)$ and therefore

$$E(\omega) = A(\omega) = 1 - R(\omega) - T(\omega). \tag{5}$$

Once the emittance is obtained, it is multiplied by Planck's power spectrum $\rho^{BB}(\omega, \beta)$, $\beta = 1/k_\mathrm{B}T$ being the thermal factor (k_B is the Boltzmann's constant), to give the power spectrum of the quasiperiodic photonic structure. In this way, the power spectrum $\rho(\omega, \beta)$ of the layered structure is given, in terms of its emittance $E(\omega)$, by

$$\rho(\omega, \beta) = E(\omega) \rho^{BB}(\omega, \beta), \tag{6}$$

with

$$\rho^{BB}(\omega, \beta) = \frac{\hbar\omega^3}{\pi^2 c^2} \frac{1}{\exp(\beta\hbar\omega - 1)}, \tag{7}$$

which is also known as Planck's law of blackbody radiation [27]. Here, c is the speed of the light in a vacuum and $\hbar$ is Planck's constant divided by 2π.

3. Numerical results

Considering the quasiperiodic multilayer structure in thermal equilibrium, with its surroundings at a given temperature T, we present now the numerical simulations for the spectral emissivity. Fundamentally, we want to know how the characteristic curve of Planck's blackbody spectrum (at a given temperature T) should be modified when we use a multilayered photonic crystal filter to model our physical system. Let us first assume an ideal case in which both the magnetic permeability and the electric permittivity can be approximated by constants, for the same frequency range of interest. The schematic geometrical representation is shown in figure 1, considering medium A as SiO_2, whose refractive index is $n_A = 1.45$, while medium B is considered to have a negative complex refractive index $n_B = -1.0 + i0.01$, i.e. it is an absorbing LHM layer which can be stimulated thermally to emit. Moreover, we assume the individual layers as quarter-wave layers, for which the quasiperiodicity is expected to be more effective [28], with central wavelength $\lambda_0 = 700$ nm. These conditions yield the physical thickness in each layer defined by the following optical relation:

$$n'_A d_A = n'_B d_B = \lambda_0/4, \tag{8}$$

where $n'_A = \mathrm{Re}(n_A)$ and $n'_B = \mathrm{Re}(n_B)$ are the real parts of n_A and n_B, respectively. The reversed phase shifts in the two layers are

$$\delta_A = (\pi/2)\Omega\cos(\theta_A), \tag{9}$$

$$\delta_B = -(\pi/2)\Omega\cos(\theta_B), \tag{10}$$

where $\Omega = \omega/\omega_0 = \lambda_0/\lambda$ is the reduced frequency and the angles θ_A and θ_B are the incidence angles that the light beam makes with the normal of the layers (z-direction in figure 1). This multilayered photonic band-gap stack is grown on an absorbing dielectric substrate characterized also by a complex refractive index $n_S = 3.0 + i0.03$, whose thickness is given by $d_S = 100\lambda_0/n'_S$, n'_S being the real part of n_S.

The thermal radiation spectra for the multilayered sequences, as a function of the reduced frequency $\Omega = \omega/\omega_0$, are depicted in figures 2(a) (periodic case), (b) (ninth generation of the Fibonacci sequence), (c) (ninth generation of the Thue–Morse sequence), and (d) (ninth generation of the double-period sequence). In all cases, we have considered the normal incidence $\theta_A = \theta_B = 0$, and $\delta_A = -\delta_B$. The temperature T is defined in terms of the midgap frequency, $\omega_0 = 2\pi c/\lambda_0$, from differentiation of Planck's law. The solid lines describe the power spectra of the multilayered structures, while the dashed curves represent the power spectra of a perfect blackbody substrate. The dotted curves are the power spectra for a non-ideal absorbing material, with complex refractive index $n_S = 3+i0.03$. Observe that Planck's curves for a perfect blackbody substrate represent the higher limit of thermal emission at multilayered sequences. In comparison with the curves related to thermal emission at a non-ideal absorbing substrate (gray-body spectrum), the stacked thin-film photonic band-gap structures arranged in a quasiperiodic way strongly alter the power spectrum of this substrate when we introduce these sequences as filters, giving rise to the so-called band-gap structures. For the periodic case (figure 2(a)) the thermal radiation spectrum presents a very soft behavior, without modulation, with low values for $\rho(\Omega)$, when compared with the quasiperiodic cases. We can observe in the range $\Omega = 1.75$–2.25, a peak of emission at around $\Omega = 2.0$.

Figure 2(b) shows the thermal radiation spectrum for the ninth sequence of the Fibonacci quasiperiodic structure for $\Omega = \omega/\omega_0$ between 0 and 2.5. The spectrum around the resonance

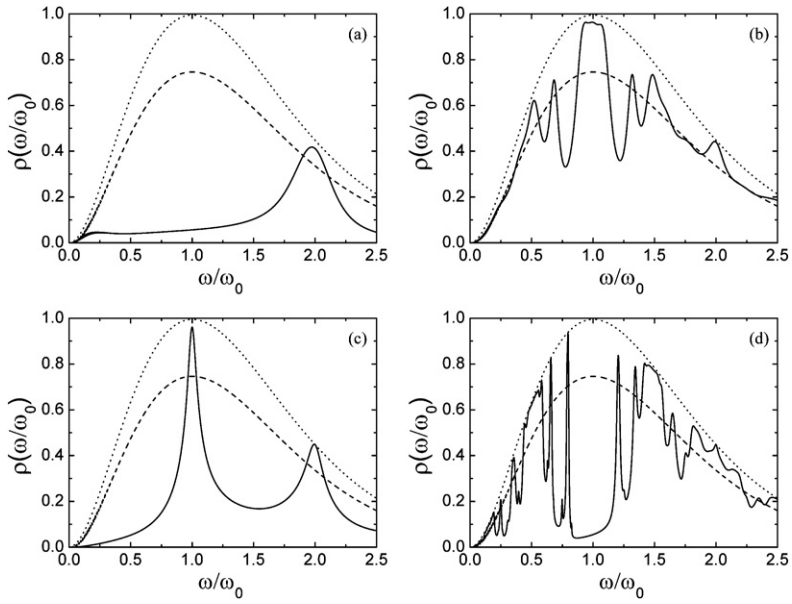

Figure 2. The thermal radiation spectra (solid lines) as a function of the reduced frequency $\Omega = \omega/\omega_0$ considering the normal incidence case, in which $n_A = 1.45$ and $n_B = -1.0 + \mathrm{i}0.01$. The photonic multilayer structure is considered to be as follows: (a) a periodic structure; (b) a ninth generation Fibonacci quasiperiodic structure; (c) a ninth generation Thue–Morse quasiperiodic structure; (d) a ninth generation double-period quasiperiodic structure. The normalized characteristic curves of Planck's thermal radiation are represented by dashed lines (the perfect blackbody), while the spectra for an absorbing material with refractive index $n_S = 3 + \mathrm{i}0.03$ are represented by dotted lines. The temperature is chosen so that the blackbody peak is aligned with the midgap frequency $\omega_0 = 2\pi c/\lambda_0$.

frequency, $\Omega = 1.0$, has a pronounced profile as compared to the periodic case depicted in figure 2(a), mainly those lying in the frequency region $0.5 < \Omega < 1.5$. The central and widest peak has a value next to $\rho(\Omega) = 0.96$, while the observed local minimum emission, next to $\Omega = 1.0$, corresponds to $\rho(\Omega) = 0.33$. If we move away from the central peak, the curve adjusts gradually towards the radiation emission profile of the gray body. In figure 2(c), we show the emission spectrum for the ninth sequence of the quasiperiodic Thue–Morse structure, whose main aspects are the presence of a narrow peak at the frequency $\Omega = 1.0$, as well as a secondary peak at $\Omega = 2.0$. Around $\Omega = 1.0$, the energy of the electromagnetic wave is strongly absorbing, resembling a light-filter, re-emitting strongly the light with $\rho(\Omega) = 0.96$. Finally, figure 2(d) shows the spectrum of emission corresponding to the ninth sequence of the double-period quasiperiodic structure. Unlike in figures 2(b) and (c), we notice a window of non-emission around $\Omega = 1.0$. The reason for this is because its transmission spectrum has a large band gap around $\Omega = 1.0$, with no counterpart with the other quasiperiodic sequences studied here or with those obtained for a multilayered system without the presence of a metamaterial [24]. Besides, the spectrum now presents a strong emission for several values of the frequency range, as we move away from the resonance frequency $\Omega = 1.0$. More importantly, as in all cases considered here, we have in figure 2(d) another constructive interference for the thermal radiation spectra at $\Omega = 2.0$.

For completeness, we have plotted in figure 3 the same situation described in figure 2, but for the positive refractive index material. For the periodic case, figure 3(a) shows a well

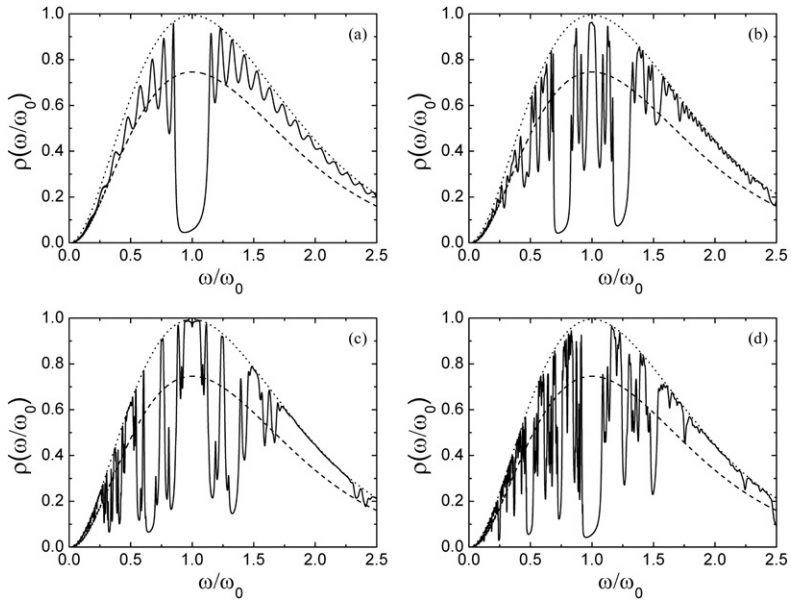

Figure 3. The same as in figure 2, but considering that medium B has a positive refractive index $n_B = 1.0 + \mathrm{i}0.01$.

defined band gap at $\Omega = 1.0$, as predicted by [26]. The thermal radiation spectra for the other quasiperiodic structures considered here, namely Fibonacci, Thue–Morse, and Double-period, are depicted in figures 3(b), (c), and (d), respectively. These figures show a similar modulation for the thermal radiation spectra found in figure 2 but with important differences, such as the fast modulation in figure 3(c) and the width of the range of low emission around $\Omega = 1.0$ in figure 3(d). Comparing them, we can conclude that the modulation of the thermal radiation spectra is not a consequence of the refractive index being negative or positive. Instead, it depends on the geometry used to characterize the system itself. Observe also that the band gap is more defined in the LHM case.

The above discussions apply only for the case where the electrical permittivity and the magnetic permeability are approximately independent of the frequency. Although, as is well known, a nondispersive medium has constant ϵ and μ, and hence zero slope, considering $n_B = -1.00 + \mathrm{i}0.01$ leads to the frequency value $\omega = 0.52\omega_\mathrm{p}$ in the model discussed below (see equations (11) and (12)). Therefore, the slopes $\mathrm{d}\epsilon(\omega)/\mathrm{d}\omega$ and $\mathrm{d}\mu(\omega)/\mathrm{d}\omega$ at this frequency ($\omega = 0.52\omega_\mathrm{p}$) are non-zero and positive, to ensure the fact that the energy of the electromagnetic wave in such a medium (which is proportional to $\mathrm{d}\epsilon(\omega)/\mathrm{d}\omega$ and $\mathrm{d}\mu(\omega)/\mathrm{d}\omega$), is always positive. Note also that we have studied the behavior of the thermal properties at frequencies close to the frequency $\omega = 0.52\omega_\mathrm{p}$. However, all realized artificial negative refractive index metamaterials have electric permittivity ϵ and magnetic permeability μ frequency dispersive to preserve the causality principle [29], being simultaneously negative only within a narrow frequency bandwidth. Since microstructures of practical negative refractive metamaterials are of the order of a few millimeters, their typical frequency region ranges from 1 to 14 GHz.

A significant change in our results can be found if one uses negative-permittivity plasma instead of negative-index medium. A dispersive medium is more realistic and it produces a very much more complex emission pattern, without self-similarity characteristics. We have

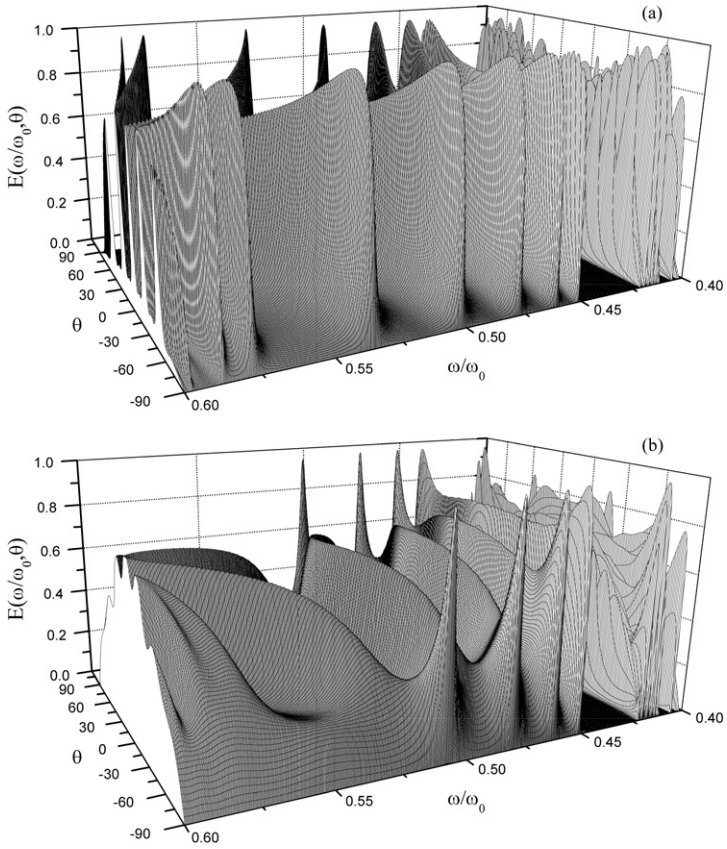

Figure 4. Emittance spectra for the periodic sequence as a function of the normalized frequency $\Omega = \omega/\omega_0$ and the incident angle θ, considering the medium B a LHM with frequency-dependent negative refractive index. (a) TE mode (s-polarized electromagnetic wave); (b) TM mode (p-polarized electromagnetic wave).

already discussed this case in a previous work [22], for the normal transmittance of light waves in a quasiperiodic multilayer with negative refractive index. The fractal pattern presented in figure 2 of that work no longer exists when we consider a frequency-dependent refractive index (figure 7(a) in that work). Therefore, a plasmonic refractive index destroys the characteristic fractal/multifractal profile of the spectrum (a pattern for quasiperiodic systems). Furthermore, as one can see from our figure 3, if the layers are composed of positive refractive index materials, we still observe the modulation (strongly influenced by the quasiperiodicity) and the band gaps.

Although we have not taken into account any free electrons in our calculation, we will use, for convenience, a causal plasmonic form for the dielectric permittivity $\epsilon(\omega)$ mimicking the Drude–Lorentz model, which can be achieved by an array of wire elements into which cuts are periodically introduced [30]. The composite material possesses a negative refractive index in the microwave region, whose corresponding dielectric permittivity $\epsilon(\omega)$ and magnetic permeability $\mu(\omega)$ are respectively given by [31]:

$$\epsilon(\omega) = 1 - \frac{\omega_{\mathrm{p}}^2}{\omega^2 + \mathrm{i}\Gamma\omega}, \tag{11}$$

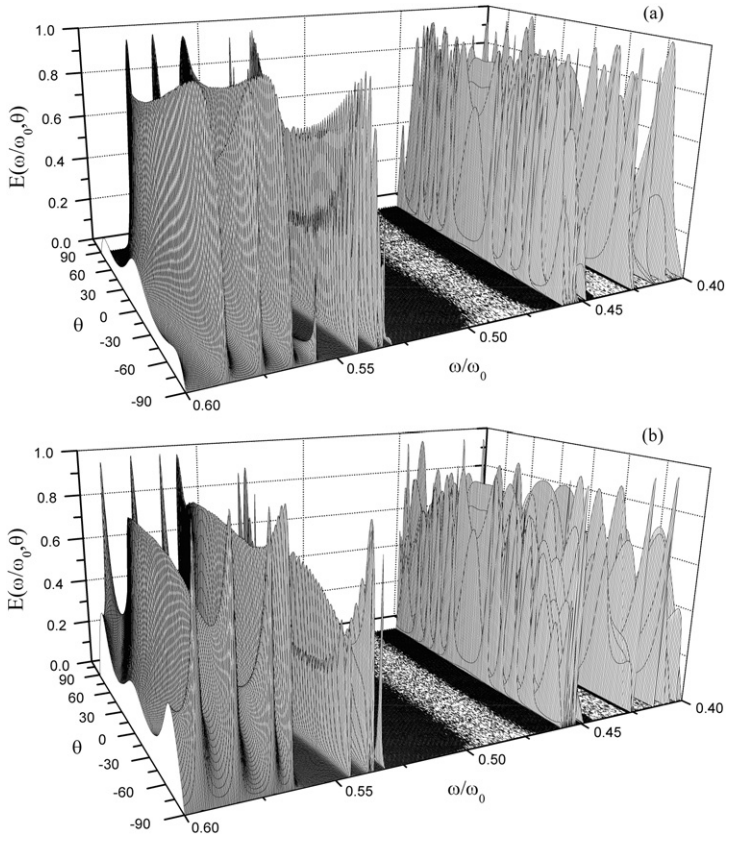

Figure 5. The same as in figure 3, but for the eighth-generation Fibonacci sequence.

$$\mu(\omega) = 1 - \frac{F\omega^2}{\omega^2 - \omega_0^2 + \mathrm{i}\Gamma\omega}, \tag{12}$$

where the plasma frequency ω_p, the resonance frequency ω_0, and the fraction F are determined only by the geometry of the lattice rather than by the charge, effective mass, and density of electrons, as is the case in naturally occurring materials. We use in this work $\omega_0/2\pi = 4$ GHz, $\omega_\mathrm{p}/2\pi = 10$ GHz, and $F = 0.56$, motivated by the experimental work of Smith and collaborators [4]. Moreover, we choose $\Gamma = 0$, a lossless material, neglecting any damping term (when lossy metamaterial is considered, the damping factor can be defined as a fraction of the plasma frequency).

Figure 4 shows the calculated emittance spectra for the periodic sequence as a function of the normalized frequency $\Omega = \omega/\omega_0$ and the incident angle θ, considering medium B a LHM with frequency-dependence negative refractive index, whose electrical permittivity and magnetic permeability are frequency dependent and defined by equations (11) and (12) for $\Gamma = 0$. We have taken into account the different polarizations, namely the TE or s-polarized mode (figure 4(a)), as well as the TM or p-polarized mode (figure 4(b)), respectively. Observe that the thermal emission peaks are here distributed symmetrically around $\theta = 0$. Besides, the angular dependence for the s-polarization case presents several band gaps, with a spectra much richer than the p-polarization case, where there is only a broad band gap lying in the region $0.45 < \Omega < 0.475$ besides a narrow gap around $\Omega = 0.48$.

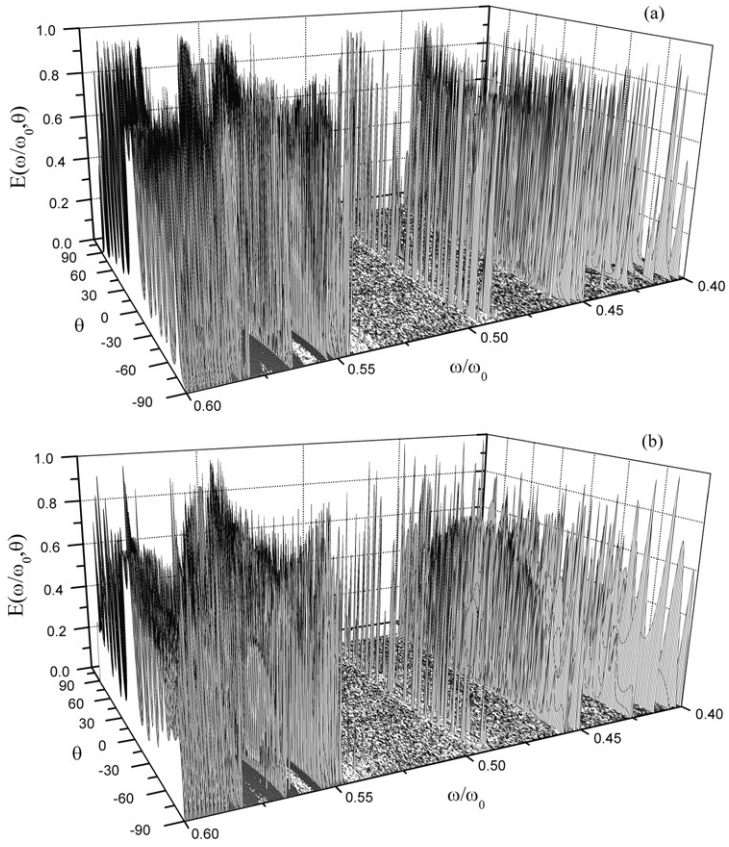

Figure 6. The same as in figure 3, but for the eighth-generation Thue–Morse sequence.

For the quasiperiodic multilayers, the emittance spectra depicted in figures 5 (eighth-generation of the Fibonacci sequence), 6 (eighth-generation of the Thue–Morse sequence), and 7 (eighth-generation of the double-period sequence) surprisingly show little dependence on the polarization of the electromagnetic wave (i.e. the s- and p-polarization cases present almost the same emittance profiles). The reason for this is because, unlike conventional dielectric materials where the electric component of the electromagnetic wave interacts more strongly with the atoms, and the magnetic component can be neglected (one-handed electromagnetic wave), in metamaterials both the electric and magnetic field interact very strongly with the atoms, giving rise to the so-called 'two-handed electromagnetic wave' [32].

Our calculation could be simplified if Lambert's law, defined as [33]

$$\log T(\omega) = A(\omega)T_0(\omega), \tag{13}$$

is applied instead of Maxwell's equations to estimate the temperature distribution of the emittance spectra, as measured in terms of the midgap frequency, $\omega_0 = 2\pi c/\lambda_0$. In the above equation, $T(\omega)$ and $T_0(\omega)$ are, respectively, the intensities of the transmitted and incident radiation at the frequency ω, and $A(\omega)$ is the absorptance defined in equation (5). However, Lambert's law is a good approximation only for a semi-infinite sample, giving different profiles for a multilayered assembly (as is the case treated here) due to the effects of wave reflection in the various interfaces [34].

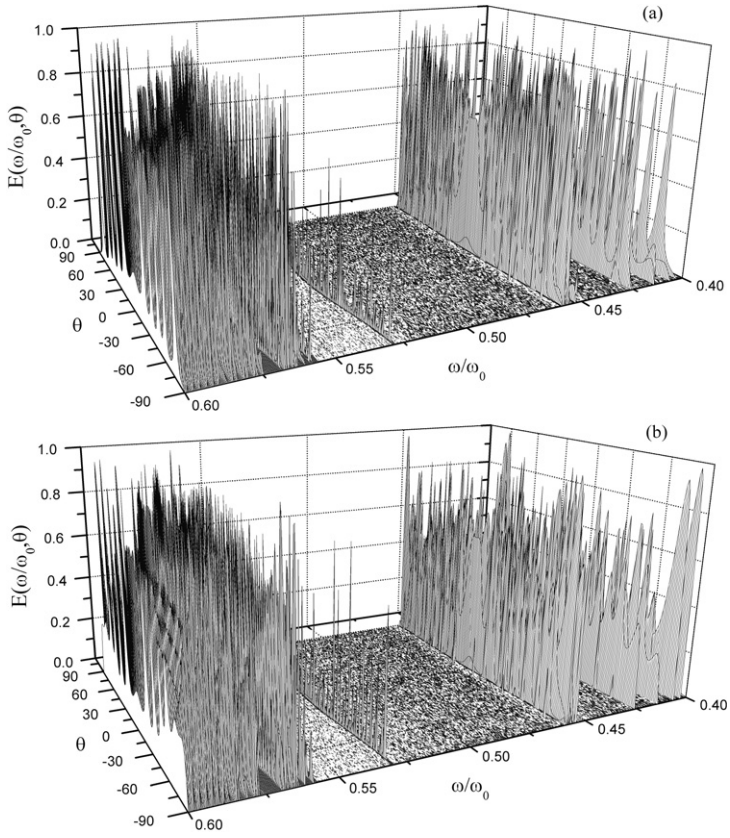

Figure 7. The same as in figure 3, but for the eighth-generation double-period sequence.

On the other hand, the periodic case shows a qualitative difference between the s- and p-polarizations, which means that the spectra are very sensitive to the geometry of the structure. Besides, the quasiperiodic photonic structures present a less soft spectrum, when compared to the periodic case, due to the higher degree of disorder. All spectra present several photonic band-gap regions, the wider one being for the double-period case in the central region $0.458 < \Omega < 0.528$.

Regarding the dependence of the emission spectra with the angle of incidence θ, also shown in figures 5–7, we can infer the following properties:

(i) all spectra are symmetrical around $\theta = 0°$, which is expected since the thermal emittance $E(\omega)$ is an even function of θ;
(ii) the thermal emittance $E(\omega)$ is null for $\theta = 90°$, meaning that we do not have propagation of the electromagnetic wave through the multilayer structure.

In general, the emittance spectrum obtained using Kirchoff's law has a higher peak if the quasiperiodic photonic structure is opaque to the electromagnetic radiation, i.e. when it behaves like a perfect blackbody. On the other hand, if the structure is not absorbent, we have a null emittance, (the energy of the electromagnetic wave is not absorbed by the structure). Qualitatively, our spectra show that the quasiperiodic sequences can block the thermal radiation, almost insensitive to the angle of incidence θ, at the following frequency range (for both polarizations):

(i) at $0.46 < \Omega < 0.53$, for the Fibonacci quasiperiodic structure (see figure 5);
(ii) at $0.46 < \Omega < 0.49$ and $0.50 < \Omega < 0.54$, for the Thue–Morse quasiperiodic structure (see figure 6);
(iii) at $0.46 < \Omega < 0.53$ and $0.54 < \Omega < 0.56$, for the double-period quasiperiodic structure (see figure 7).

Therefore, the quasiperiodic multilayer structures is a much better candidate for designing efficient LHM filters, when compared to their periodic counterpart depicted in figure 4 (see also [21, 26]).

4. Conclusions

In this work, we have investigated the thermal behavior of light waves considering quasiperiodic multilayered structures, namely those obeying the recursion relation which defines the Fibonacci, Thue–Morse, and double-period sequences. They can be used to enhance, suppress or attenuate spontaneous emission in all or certain directions by changing the density of modes, and therefore behaving as filters for modification of Planck's blackbody spectrum, considering that one of their components has a negative refractive index. Initially, we calculated the thermal spectra for the ideal case in which both the electric permittivity and the magnetic permeability can be considered as constants, revealing interesting photonic band-gap structures. For a more realistic case, taking into account the frequency-dependent electric permittivity ϵ and magnetic permeability μ to characterize the negative refractive index n in layer B, we have studied the spectral emissivity for oblique incidence, considering both the s- and p-polarization of the electromagnetic wave. For the periodic case, the thermal emission spectra is symmetrically distributed around $\theta = 0$, with significant differences for the s- and p-polarization cases. Moreover, the quasiperiodic thermal spectra is insensitive to light polarization with a broad band gap in the central frequency region.

Acknowledgments

We would like to thank partial financial support from the Brazilian Research Agencies CNPq (projects CT-ENERG 554889/2006-4 and CNPq-Rede NanoBioestruturas 555183/2005-0), Finep and FAPEMA.

References

[1] Veselago V G 1968 *Sov. Phys.—Usp.* **10** 509
[2] Pendry J B, Holden A J, Robbins D J and Stewart W J 1998 *J. Phys.: Condens. Matter* **10** 4785
Pendry J B, Holden A J, Robbins D J and Stewart W J 1999 *IEEE Trans. Microw. Theory Tech.* **47** 2075
[3] Pendry J B 2000 *Phys. Rev. Lett.* **85** 3966
[4] Smith D R, Padilla W J, Vier D C, Nemat-Nasser S C and Schultz S 2000 *Phys. Rev. Lett.* **84** 4184
[5] Shelby R A, Smith D R and Shultz S 2001 *Science* **292** 77
[6] Wang L J, Kuzmich A and Doragiu A 2000 *Nature* **406** 277
[7] Dolling G, Enkrich C, Wegener M, Soukoulis C M and Linden S 2006 *Science* **312** 892
[8] Soukoulis C M, Kafesaki M and Economou E N 2006 *Adv. Mater.* **18** 1941
[9] Tassin P, Veretennicoff I and Van der Sande G 2006 *Opt. Commun.* **264** 130
[10] Engheta N 2002 *IEEE Antennas Wireless Propag. Lett.* **1** 10
[11] Agranovich V M and Gartstein Y N 2006 *Phys.—Usp.* **49** 1029
[12] de Medeiros F F, Albuquerque E L and Vasconcelos M S 2005 *Microelectron. J.* **36** 1006
[13] Veselago V G and Narimanov E E 2006 *Nat. Mater.* **5** 759
[14] Wiltshire K C M *et al* 2001 *Science* **291** 849

[15] Parazzoli C G *et al* 2004 *Appl. Phys. Lett.* **95** 3232
[16] Ramakrishna S A 2005 *Rep. Prog. Phys.* **68** 449
[17] Houck A, Brock J B and Chuang I L 2003 *Phys. Rev. Lett.* **90** 137401
[18] Joannopoulos J D, Meade R D and Winn J N 1995 *Photonic Crystals: Molding the Flow of Light* (Princeton, NJ: Princeton University Press)
[19] Smith D R, Pendry J B and Wiltshire M C K 2004 *Science* **305** 788
[20] Kästel J and Fleischhauer M 2005 *Phys. Rev.* A **71** 01180
Kästel J and Fleischhauer M 2005 *Laser Phys.* **15** 1
[21] Maksimović M and Jaksić Z 2005 *Phys. Lett.* A **342** 497
Maksimović M and Jaksić Z 2006 *J. Opt. A: Pure Appl. Opt.* **8** 355
[22] Albuquerque E L and Cottam M G 2004 *Polaritons in Periodic and Quasiperiodic Structures* (Amsterdam: Elsevier)
[23] Albuquerque E L and Cottam M G 2003 *Phys. Rep.* **376** 225
Vasconcelos M S and Albuquerque E L 1999 *Phys. Rev.* B **59** 11128
[24] de Medeiros F F, Albuquerque E L and Vasconcelos M S 2006 *J. Phys.: Condens. Matter* **18** 8737
[25] Pigeat P, Rouzel D and Weber B 1998 *Phys. Rev.* B **57** 9293
[26] Cornelius C M and Dowling J P 1999 *Phys. Rev.* A **59** 4736
[27] Planck M 1959 *The Theory of Heat Radiation* (New York: Dover)
[28] Kono K, Nakada S, Narahara Y and Ootuka Y 1991 *J. Phys. Soc. Japan* **60** 368
[29] Ziolkowski R W and Heyman E 2001 *Phys. Rev.* E **64** 056625
[30] Pendry J B and Smith D R 2004 *Phys. Today* **57** (6) 37
[31] Shadrivov H V, Sukhorukov A A and Kivshar Y S 2003 *Appl. Phys. Lett.* **82** 3820
[32] Vladimir S M 2007 *Nature* **1** 41
[33] Atkins P W 1994 *Physical Chemistry* (Oxford: Oxford University Press)
[34] Ayappa K G, Davis H T, Crapiste G, Davis E A and Gordon J 1991 *Chem. Eng. Sci.* **46** 1005